THE JOURNAL OF PHYSICAL CHEMISTRY A

pubs.acs.org/JPCA Article

A Conceptual DFT Study of Phosphonate Dimers: Dianions Supported by H-Bonds

Published as part of The Journal of Physical Chemistry virtual special issue "Paul Geerlings Festschrift".

Luis Miguel Azofra,* José Elguero, and Ibon Alkorta*

Cite This: *J. Phys. Chem. A* 2020, 124, 2207−2214 Read Online

ACCESS | Metrics & More | Article Recommendations | Supporting Information

ABSTRACT: A conceptual DFT study of the dissociation of anionic and neutral phosphonate dimers has been carried out. In addition, the dianion complexes have been studied in the presence of two solvents, water and tetrahydrofuran. The dissociation of the dianion complexes in the gas phase and in solution present a maximum along the reaction coordinate that is not present in the neutral−neutral and anion−neutral complexes. The principal chemical descriptors (chemical potential, reaction electronic flux, hardness, and global electrophilicity index) do not show changes in their trends along the dissociation profiles even when there is an energy maximum in the case of the anion−anion complexes.

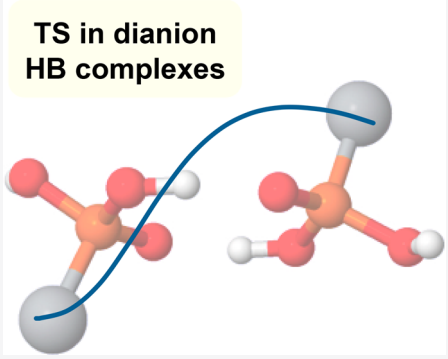

INTRODUCTION

Nowadays, there are no doubts about the importance of the noncovalent interactions for the understanding of the behavior and properties of molecules in biological, environmental, and materials sciences. In the last years, newcomers to the field of noncovalent interactions have been described[1] and named based on those atoms directly involved in the interaction as Lewis acids (halogen,[2−4] chalcogen,[5−7] pnitcogen,[8−10] tetrel,[11−13] triel,[14,15] coinaged,[16] beryllium,[17,18] lithium,[19] and aerogen[20] bonds). Although hydrogen bonds (H-bonds),[21,22] already described a century ago,[23,24] remain as the most important and studied[25] weak bond, from time to time new findings appear that challenge our view about this fundamental chemical entity.

One of the latest findings is the possibility to find minima between molecules with the same charge (cation−cation or anion−anion) in gas phase. The strong repulsive electrostatic effect should prevent the presence of such minima; however, in 2005, Kass showed computationally that dianion complexes formed by carboxylates (derived from oxalic, malonic, terephthalic, and glycine, among others) could be stable in the gas phase and that an energy barrier prevented them from dissociation.[26] More recently, in 2012, Espinosa and coworkers explored phosphate−phosphate electrostatically defying complexes in the gas phase.[27] They extended this study to the effect of the environment on the complexes,[28] and they also analyzed oxoanion-based hydrogen-bonded complexes,[29] rationalized the interaction in carboxylic acid dimers of anions and cations with different distances between the charged groups,[30] and studied the cation−cation complexes formed by nucleic acids in Watson−Crick disposition.[31] Other authors have extended the computational studies on complexes stabilized by hydrogen-bonding interactions.[32−39] In addition, other interactions such as halogen bonds have been used to maintain together the two interacting charged molecules.[35,40−44]

At experimental level, the use of anion receptors has been employed to disperse the charge of the anions and reduce the electrostatic repulsion when the two anions approach one to each other. Using this methodology, dimers of dihydrogen phosphate anions,[45−48] bisulfates,[49,50] organic phosphates,[51] pyrophosphates,[52] and phosphonates[53] have been characterized.

Conceptual DFT (CDFT)[54] offers a series of theoretical tools that allow an analysis of the intrinsic reactivity for chemical events occurring at the electronic level and being directly associated with physicochemical properties of both global and local nature. A detailed explanation of the Conceptual DFT descriptors can be found in the very rich literature on the subject, among which we highlight some of our works in the field.[55−57] Notwithstanding, it is convenient to proceed with a brief review of those main descriptors that

Received: November 14, 2019
Revised: February 22, 2020
Published: February 24, 2020

https://dx.doi.org/10.1021/acs.jpca.9b10681
J. Phys. Chem. A 2020, 124, 2207−2214

we will use in the present article. When the energy of a given chemical process is represented along the intrinsic reaction coordinate (IRC or ξ), the ξ_R, ξ_{TS}, and ξ_P values represent the points of the IRC in which are located reactant (R), transition state (TS), and product (P), respectively. Since these species are stationary points along the potential energy surface (PES), the reaction force, F,[58−60] defined as the as the negative first derivative of the energy with respect to ξ, should be zero (eq 1):

$$F(\xi) = -dE/d\xi = 0 \text{ (for R, TS, and P)} \quad (1)$$

In addition to the energy and the reaction force, the electronic chemical potential, μ,[61,62] (eq 2) and its first derivative with respect to ξ, J (reaction electronic flux or REF; eq 3),[63] will be analyzed:

$$\mu \approx (\varepsilon_L + \varepsilon_H)/2 \quad (2)$$

$$J(\xi) = -d\mu/d\xi \quad (3)$$

Here ε_L and ε_H refer to the energy of the lowest-unoccupied and highest-occupied frontier orbitals, respectively. Finally, the chemical hardness, η,[61,62] (eq 4) and the global electrophilicity index, ω,[64,65] (eq 5) will be also examined:

$$\eta \approx \varepsilon_L - \varepsilon_H \quad (4)$$

$$\omega \approx \mu^2/2\eta \quad (5)$$

Thus, in this article, the dissociation profile of organic phosphonate dimers (Figure 1) in neutral and anionic forms

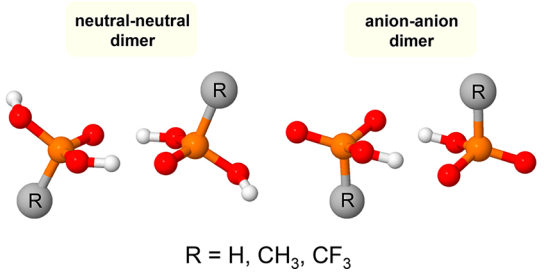

Figure 1. Neutral−neutral and anion−anion phosphonate dimers studied.

have been studied in gas phase by means of the Conceptual DFT approach. For some selected cases, the effect of the solvent has been studied via the COSMO model using the standard parameters for water and tetrahydrofuran (THF). In order to analyze the nature of the interactions holding the aforementioned dimers, energy results and selected reactivity descriptors have been compared. Herein, we report the presence of unusual saddle points that result from the dissociation of interanionic H-bond (IAHB) complexes that behave as "ghost TSs" based on the atypical behavior of their chemical descriptors.

COMPUTATIONAL METHODS

The dissociation profiles of selected organic phosphonate dimers in neutral and anionic forms have been studied through the use of Density Functional Theory (DFT) via the spin-restricted Kohn−Sham (RKS) formalism and the M06-2X functional,[66] using the 6-311+G(d) basis set.[67] In all cases, the phosphorus−phosphorus distance has been used as intrinsic reaction coordinate (IRC = ξ) with a step-size of 0.1 Å and separating monomers until a P···P distance of 6.5−7.0 Å. Frequency calculations were performed to confirm the nature of the stationary points (minima or first-order transition states with one imaginary frequency). Both optimization and frequency calculations were performed using a fine grid. For selected cases and to simulate the solvent effects, the COSMO model[68] has been used with the standard parameters for water and tetrahydrofuran (THF). All calculations were carried out through the facilities provided by the NWChem[69] package.

RESULTS AND DISCUSSION

The phosphonic acid function possesses two acidic protons featuring, for instance, a first pK_a at 2.12 and the second pK_a at 7.29 when R is the methyl group.[70] Dimers of phosphonates are structures connected by H-bonds between the constituted monomers. The H-bonds induce chirality in each of the phosphonate molecules involved in the interaction.[71] According to the disposition of the R groups (Figure 2), two minima can be described based on symmetry: C_2 (pointing toward the same plane) and C_i (pointing toward different planes), which correspond to homochiral and heterochiral dimers, respectively.[72,73] In the case of the anion−anion phosphonate dimers, complexes with C_i symmetry are more favored than those with C_2 symmetry by 0.12, 0.16, 0.14 kcal mol^{-1}, for R = H, CH_3, CF_3, respectively. Preliminary tests at the MP2/6-31+G(d,p) level of theory have also corroborated the higher stability of the C_i dimers, *e.g.*, C_i $(CH_3HPO_3^-)_2$ dimer is 0.58 kcal mol^{-1} more stable than the C_2 one. For simplicity, the Conceptual DFT analysis will be circumscribed to the C_i dimers for both neutral−neutral and anion−anion phosphonate complexes.

The $(H_2PO_3^-)_2$ dimer in gas phase is characterized by the presence of two OH···O$^-$ H-bonds with identical interatomic O···H distances of 1.69 Å. Its dissociation profile (Figure 3a), representing the electronic binding energy vs. the interatomic distance of the two phosphorus atoms (intrinsic reaction coordinate), indicates that, at R(P···P) = 5.84 Å, a maximum is observed with relative energy of 10.19 kcal mol^{-1}. This is corroborated by the representation of the reaction force (Figure 3a), in which, at R(P···P) = 5.84 Å, F = 0 kcal mol^{-1} Å^{-1}, that is, indicating the presence of a stationary point associated with a transition state. Similarly, gas phase neutral $(H_3PO_3)_2$ dimer exhibits two OH···O H-bonds with interatomic O···H distances of 1.62 Å; however, its dissociation profile (Figure 3b) clearly indicates the nonexistence of any maximum. The reaction force (Figure 3b) also corroborates this, since at longer P···P distances of the reaction coordinate the force asymptotically tends to zero. This behavior indicates that neutral phosphonate dimers do not exhibit any TS during its dissociation: the longest separation of the monomers, the lowest binding energy, with a value of zero at infinite distance. On the contrary, anionic phosphonate dimers (charge −2), exhibit a TS that prevent them from dissociation with reachable electronic barriers between 10 and 15 kcal mol^{-1} for the cases under study.

These unique features are also corroborated when comparing neutral $(RH_2PO_3)_2$ and anionic $(RHPO_3^-)_2$ phosphonate dimers for R = CH_3 or CF_3. Specifically, for $(CH_3HPO_3^-)_2$ and $(CF_3HPO_3^-)_2$ cases (Figure 3, parts c and d), a maximum is found at interatomic phosphorus distances of 5.86 and 6.06 Å and relative energies of 11.63 and 12.68 kcal mol^{-1}, respectively. An *ab initio* exploration of the dissociation profile of these interanionic H-bond (IAHB) complexes reveals that the presence of the TS is not a DFT artifact. As seen in

https://dx.doi.org/10.1021/acs.jpca.9b10681
J. Phys. Chem. A 2020, 124, 2207−2214

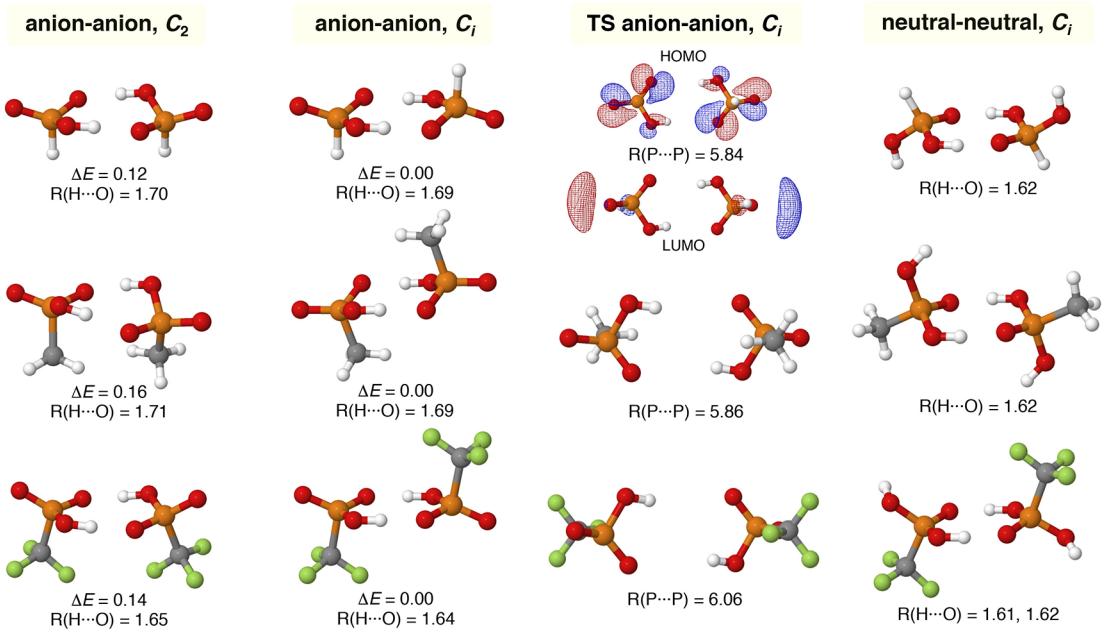

Figure 2. Structures and relative electronic energies (in kcal mol^{-1}) of the C_2 and C_i anion−anion phosphonate complexes for R = H, CH_3, and CF_3 and corresponding C_i anion−anion TSs and neutral−neutral dimers. Notes: selected H-bond distances are shown in Å. For those cases in which R = CF_3, minima acquire C_1 symmetry since C_2 and C_i complexes exhibit small imaginary frequencies. HOMO and LUMO are indicated in TS for $(H_2PO_3^-)_2$ dimer.

Figure S1 from the Supporting Information, the dissociation of the $(H_2PO_3^-)_2$ dimer in gas phase has been also studied at the MP2/6-311++G(d,p) level of theory (including diffuse and polarization functions for all atoms), corroborating the presence of such maximum at R(P···P) = 5.84 Å, and obtaining similar energy results as at the M06-2X/6-311+G(d) level.

An interesting characteristic found in the binding electronic energy of gas phase dianionic phosphonate dimers is its positive value proper of nonfavored processes. For the $(H_2PO_3^-)_2$, $(CH_3HPO_3^-)_2$, and $(CF_3HPO_3^-)_2$ cases, values of 31.28, 29.78, and 25.22 kcal mol^{-1} are respectively obtained (the less positive, the more electron withdrawing substituent is R). By comparison, the dissociation profiles of $(CH_3HPO_3^-)_2$ in water and THF solutions analyzed via the COSMO solvation model (Figure 3, parts e and f) show the existence of favored binding electronic energies of −15.51 and −10.92 kcal mol^{-1} as well as the presence of a maximum at 5.78 and 5.83 Å with relative barriers of 15.36 and 14.64 kcal mol^{-1}, respectively. An important question arises in what concern to the behavior of dianionic phosphonate dimers in solution: does this maximum obey to a real TS or to a DFT artifact? As seen in Figure 3, parts e and f, the existence of a maximum in these dissociation profiles is unquestionable although with a smoother evolution toward products. This might suggest that this behavior is characteristic of dianionic phosphonate dimers regardless the sign of the binding electronic energy, or in other words, regardless the medium in which they are. Notwithstanding, despite all our attempts to optimize the aforementioned saddle points in solution, we were totally unable to describe the respective TSs with an imaginary frequency characterizing the formation-dissociation of the monomers. On the contrary, optimization of the maximum derived from the dissociation profile of $(H_2PO_3^-)_2$ dimer in gas phase leads to a clear saddle point with an imaginary frequency of 59i, with similar values for the analogous TSs of $(CH_3HPO_3^-)_2$ and $(CF_3HPO_3^-)_2$ dimers in vacuum. Despite this issue, it seems reasonable to assume that the solvent effect tends to remove the dissociation barrier of dianions dimers, *i.e.*, making the IAHB complexes behave like neutral dimers.

An exploration of the anion−neutral complexes of phosphonates revealed the existence of C_1-symmetrized H-bounded complexes. Figure 4(a) gathers the structures of the $RHPO_3^-\cdots RH_2PO_3$ anion−neutral complexes when R = H, CH_3, CF_3. Contrasting with dianion and neutral dimers, the anionic moiety in the anion−neutral complex acts as Lewis base, while the neutral moiety is acting as H-bond donor via their acidic hydrogen atoms. In the three cases, large negative binding energies have been computed, with values of −44.78, −42.69, and −47.20 kcal mol^{-1}, respectively, and interatomic O···H distances close to 1.6 Å, indicating that these interactions are highly stable.

An analysis of the dissociation profiles indicates that anionic and neutral units are regrouped at a given phosphorus−phosphorus distance. Thus, at R(P···P) = 4.8 Å, the two acidic hydrogen atoms in the neutral moiety point toward only one O atom in the anionic moiety (Figure 4a, structure in parentheses). The dissociation profile shown at Figure 4b, clearly indicate that anion−neutral complexes behave like neutral dimers, *i.e.*, unlike dianion dimers, they do not exhibit a TS that prevent them from dissociation.

Given the existence of TSs in anionic $(RHPO_3^-)_2$ phosphonate dimers, one would expect changes in the chemical descriptors as it is general in any chemical reaction. Both, chemical potential and reaction electronic flux normally exhibit a changing behavior, with deviations taking place at (or very close to) the characteristic ξ_R, ξ_{TS}, and ξ_P points or at ξ_1 and ξ_2, which are associated with the minimum and maximum of the reaction force profile. For example, this is the case of the hemiacetal formation in sugar's models (formaldehyde plus methanol),[55] in which big changes are seen for μ and REF in regions of the IRC close to a minimum or a maximum state. Very interestingly and despite the presence of the TSs, anionic

https://dx.doi.org/10.1021/acs.jpca.9b10681
J. Phys. Chem. A 2020, 124, 2207−2214

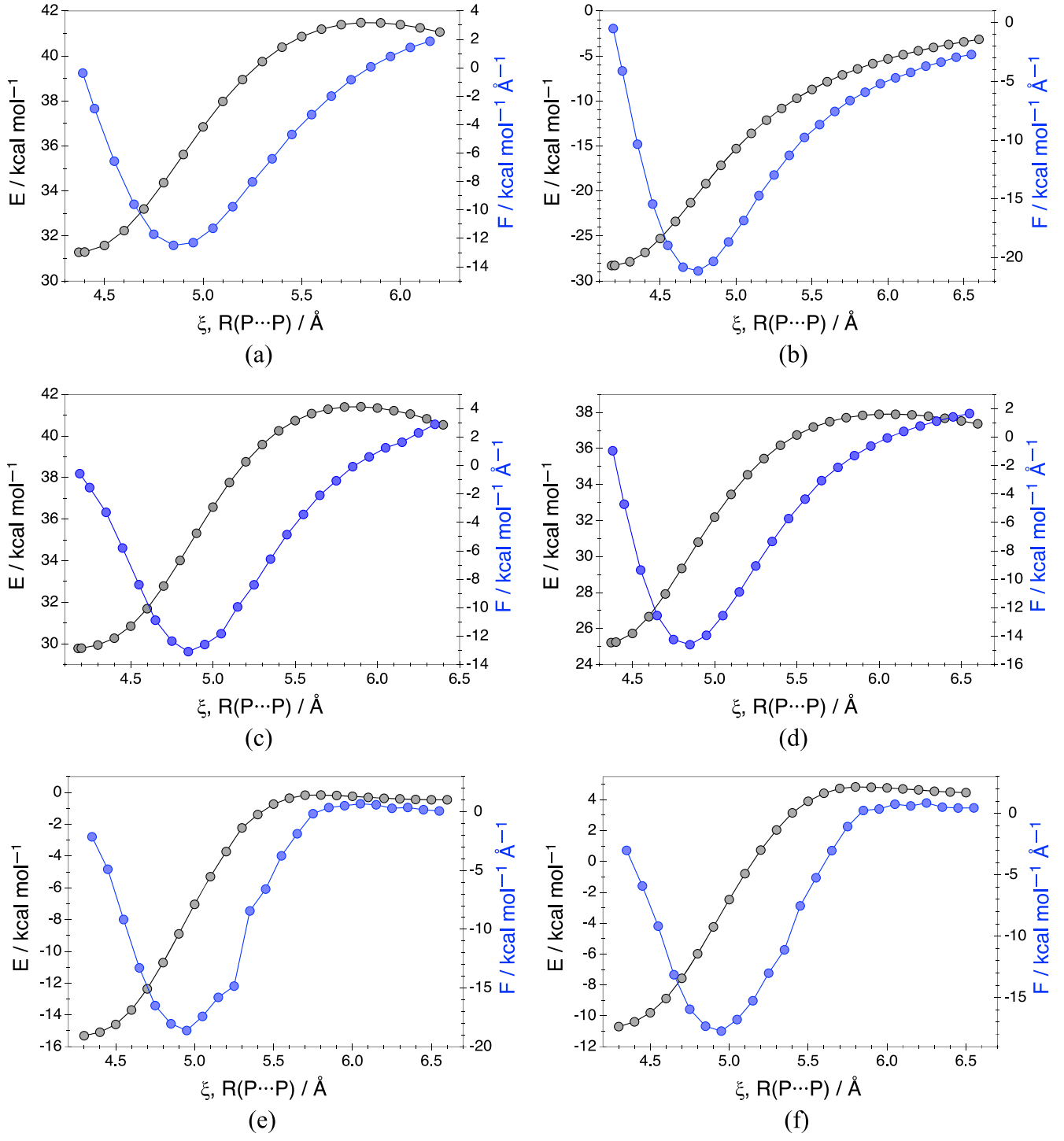

Figure 3. Electronic energy (black, binding, kcal mol^{-1}) and reaction force (blue, kcal mol^{-1} Å^{-1}) profiles vs. P···P distance (IRC, Å) for the following: (a) anionic $(H_2PO_3^-)_2$; (b) neutral $(H_3PO_3)_2$; (c) anionic $(CH_3HPO_3^-)_2$; (d) anionic $(CF_3HPO_3^-)_2$ phosphonate dimers in gas phase; anionic $(CH_3HPO_3^-)_2$ phosphonate dimers (e) in water and (f) in THF solutions.

$(RHPO_3^-)_2$ phosphonate dimers do not exhibit any changing activity in both properties. As seen at Figure 5a for $(H_2PO_3^-)_2$ dimer, its chemical potential profile displays a decreasing linear behavior without any remarkable change of tendency both along the reactant area or once passed the TS. The longest is the interatomic phosphorus distance the smallest is the chemical potential, without any electronic change around the TS area. Differences of *ca.* 10−12 kcal mol^{-1} are seen for $\Delta\mu$ between ξ_{TS} and ξ_R (see also Figure 5, parts b and c) for the three cases of $(RHPO_3^-)_2$ phosphonate dimers, being R = H, CH_3, and CF_3. For the case of the REF profiles, they exhibit positive values along all the range (proper of nonspontaneous electronic rearrangements) but do not start and reach the zero-flux regime as it is expected for minima and do not show any change in the TS regions as it is expected for maxima. Since the chemical potential monotonically decreases along the reaction

https://dx.doi.org/10.1021/acs.jpca.9b10681
J. Phys. Chem. A 2020, 124, 2207−2214

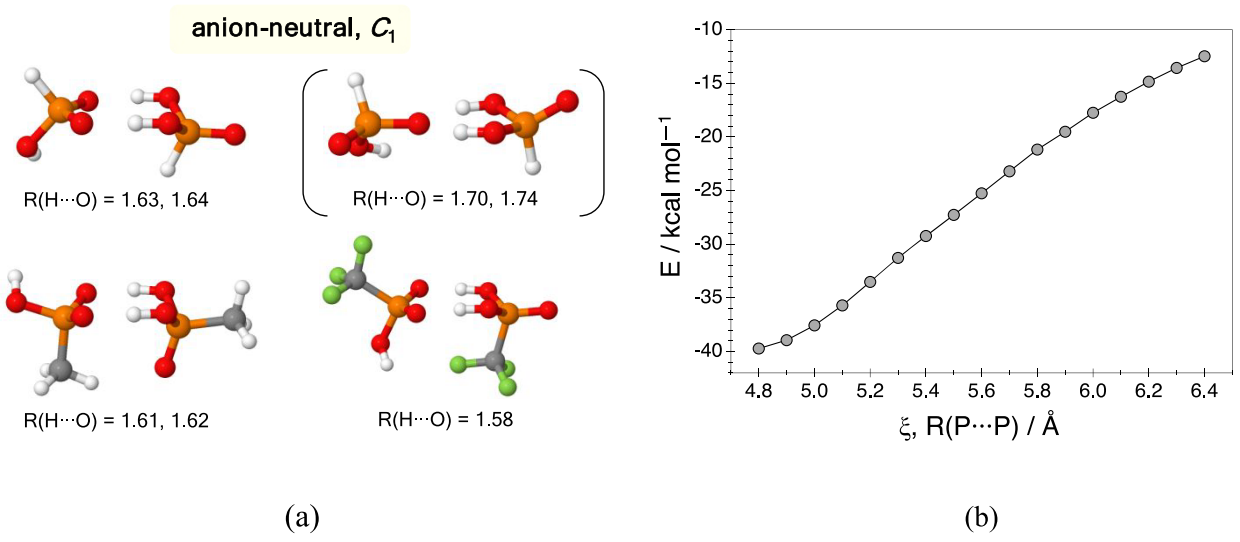

Figure 4. (a) Structures for anion−neutral phosphonate complexes for R = H, CH_3, and CF_3, with selected H-bond distances shown in Å, and (b) electronic energy (binding, kcal mol^{-1}) profile vs. P···P distance (IRC, Å) for the $H_2PO_3^-$···H_3PO_3 complex.

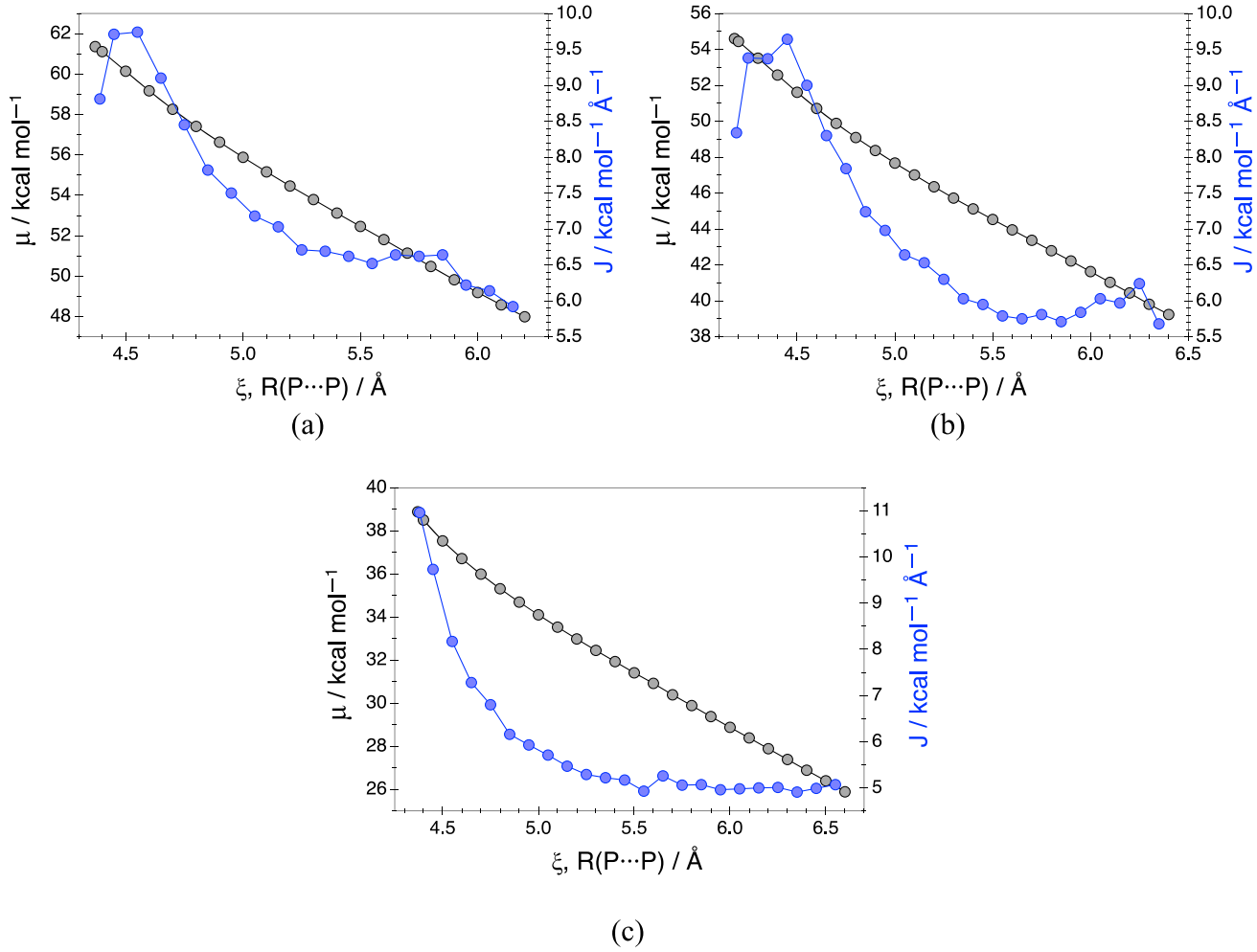

Figure 5. Chemical potential (kcal mol^{-1}) and reaction electronic flux (kcal mol^{-1} Å^{-1}) profiles vs. P···P distance (IRC, Å) for anionic (a) $(H_2PO_3^-)_2$, (b) $(CH_3HPO_3^-)_2$, and (c) $(CF_3HPO_3^-)_2$ phosphonate dimers in the gas phase.

coordinate, it is expected that REF remains almost constant and without great deviations. This tendency is also seen for $(CH_3HPO_3^-)_2$ phosphonate dimer in water and THF solution, in which μ displays an almost linear decreasing behavior. Changes in the REF are less than 5 kcal mol^{-1} Å^{-1} in all the range of P···P distances making difficult an accurate

https://dx.doi.org/10.1021/acs.jpca.9b10681
J. Phys. Chem. A 2020, 124, 2207−2214

interpretation for this case, beyond establishing that the proximity to the zero-flux regime is due to the favorable interactions taking place in solution.

An analysis of the chemical hardness reveals that its profile along the IRC exhibits a linear increasing behavior (see Figure S2 from the Supporting Information). Since the electrophilicity index is directly related with the hardness and the chemical potential, it is expected that its profile also evolves monotonically along the reaction coordinate (Figure S2) without any remarkable change in the TS area. In addition, the longer phosphorus interatomic distance the higher hardness and the smaller electrophilicity, being in consonance with the maximum hardness principle.[74]

CONCLUSIONS

Considering these data, we can conclude that dianionic phosphonate dimers (charge −2) exhibit a TS during its dissociation which is not present in their related neutral−neutral (charge 0) and neutral-anionic (charge −1) stable complexes. Contrary to classical chemical processes, this saddle point behaves as a "ghost TS", exhibiting no trend changes of their principal chemical descriptors, namely chemical potential and reaction electronic flux, but also hardness and global electrophilicity index. As far as we know, this represents an atypical case in the description of chemical reactions in terms of Conceptual DFT, and we hope our findings stimulate further interest in the understanding of these uncommon systems.

ASSOCIATED CONTENT

Supporting Information

The Supporting Information is available free of charge at https://pubs.acs.org/doi/10.1021/acs.jpca.9b10681.

Electronic energy and reaction force profiles, hardness and global electrophilicity index, HOMO and LUMO frontier orbitals, and optimized Cartesian coordinates (PDF)

AUTHOR INFORMATION

Corresponding Authors

Luis Miguel Azofra − *CIDIA-FEAM (Unidad Asociada al Consejo Superior de Investigaciones Científicas, CSIC, avalada por el Instituto de Ciencia de Materiales de Sevilla, Universidad de Sevilla), Instituto de Estudios Ambientales y Recursos Naturales (i-UNAT) and Departamento de Química, Universidad de Las Palmas de Gran Canaria (ULPGC), 35017 Las Palmas de Gran Canaria, Spain;* orcid.org/0000-0003-4974-1670; Email: luismiguel.azofra@ulpgc.es

Ibon Alkorta − *Instituto de Química Médica (IQM-CSIC), E-28006 Madrid, Spain;* orcid.org/0000-0001-6876-6211; Email: ibon@iqm.csic.es

Author

José Elguero − *Instituto de Química Médica (IQM-CSIC), E-28006 Madrid, Spain;* orcid.org/0000-0002-9213-6858

Complete contact information is available at: https://pubs.acs.org/10.1021/acs.jpca.9b10681

Notes

The authors declare no competing financial interest.

ACKNOWLEDGMENTS

L.M.A. is an ULPGC Postdoc Fellow, and thanks Universidad de Las Palmas de Gran Canaria (ULPGC) for support. J.E. and I.A. acknowledge the Ministerio de Ciencia, Innovación y Universidades (PGC2018-094644−B-C22), and Comunidad Autónoma de Madrid (P2018/EMT-4329 AIRTEC-CM) for financial support. Gratitude is also due to the KAUST Supercomputing Laboratory using the supercomputer Shaheen II and CTI (CSIC) for providing the computational resources.

REFERENCES

(1) Legon, A. C. Tetrel, pnictogen and chalcogen bonds identified in the gas phase before they had names: a systematic look at non-covalent interactions. *Phys. Chem. Chem. Phys.* **2017**, *19* (23), 14884−14896.

(2) Wolters, L. P.; Schyman, P.; Pavan, M. J.; Jorgensen, W. L.; Bickelhaupt, F. M.; Kozuch, S. The many faces of halogen bonding: a review of theoretical models and methods. *Wiley Interdiscip. Rev. Comput. Mol. Sci.* **2014**, *4* (6), 523−540.

(3) Cavallo, G.; Metrangolo, P.; Milani, R.; Pilati, T.; Priimagi, A.; Resnati, G.; Terraneo, G. The Halogen Bond. *Chem. Rev.* **2016**, *116* (4), 2478−2601.

(4) Kolář, M. H.; Hobza, P. Computer Modeling of Halogen Bonds and Other σ-Hole Interactions. *Chem. Rev.* **2016**, *116* (9), 5155−5187.

(5) Minyaev, R. M.; Minkin, V. I. Theoretical study of O - > X (S, Se, Te) coordination in organic compounds. *Can. J. Chem.* **1998**, *76* (6), 776−788.

(6) Sanz, P.; Yáñez, M.; Mó, O. Resonance-Assisted Intramolecular Chalcogen−Chalcogen Interactions? *Chem. - Eur. J.* **2003**, *9* (18), 4548−4555.

(7) Wang, W.; Ji, B.; Zhang, Y. Chalcogen Bond: A Sister Noncovalent Bond to Halogen Bond. *J. Phys. Chem. A* **2009**, *113* (28), 8132−8135.

(8) Scheiner, S. A new noncovalent force: Comparison of P···N interaction with hydrogen and halogen bonds. *J. Chem. Phys.* **2011**, *134* (9), 094315.

(9) Zahn, S.; Frank, R.; Hey-Hawkins, E.; Kirchner, B. Pnicogen Bonds: A New Molecular Linker? *Chem. - Eur. J.* **2011**, *17* (22), 6034−6038.

(10) Del Bene, J. E.; Alkorta, I.; Elguero, J. The Pnicogen Bond in Review: Structures, Binding Energies, Bonding Properties, and Spin-Spin Coupling Constants of Complexes Stabilized by Pnicogen Bonds. *Noncovalent Forces* **2015**, *19*, 191−263.

(11) Alkorta, I.; Rozas, I.; Elguero, J. Molecular Complexes between Silicon Derivatives and Electron-Rich Groups. *J. Phys. Chem. A* **2001**, *105* (4), 743−749.

(12) Bauzá, A.; Mooibroek, T. J.; Frontera, A. Tetrel-Bonding Interaction: Rediscovered Supramolecular Force? *Angew. Chem., Int. Ed.* **2013**, *52* (47), 12317−12321.

(13) Grabowski, S. J. Tetrel bond−σ-hole bond as a preliminary stage of the SN2 reaction. *Phys. Chem. Chem. Phys.* **2014**, *16* (5), 1824−1834.

(14) Grabowski, S. J. Triel Bonds, π-Hole-π-Electrons Interactions in Complexes of Boron and Aluminium Trihalides and Trihydrides with Acetylene and Ethylene. *Molecules* **2015**, *20* (6), 11297−11316.

(15) Bauzá, A.; García-Llinás, X.; Frontera, A. Charge-assisted triel bonding interactions in solid state chemistry: A combined computational and crystallographic study. *Chem. Phys. Lett.* **2016**, *666*, 73−78.

(16) Legon, A. C.; Walker, N. R. What's in a name? 'Coinage-metal' non-covalent bonds and their definition. *Phys. Chem. Chem. Phys.* **2018**, *20* (29), 19332−19338.

(17) Yáñez, M.; Sanz, P.; Mó, O.; Alkorta, I.; Elguero, J. Beryllium Bonds, Do They Exist? *J. Chem. Theory Comput.* **2009**, *5* (10), 2763−2771.

(18) Montero-Campillo, M. M.; Mó, O.; Yáñez, M.; Alkorta, I.; Elguero, J. Chapter Three - The beryllium bond. *Adv. Inorg. Chem.* **2019**, *73*, 73−121.
(19) Solimannejad, M.; Ghafari, S.; Esrafili, M. D. Theoretical insight into cooperativity in lithium-bonded complexes: Linear clusters of LiCN and LiNC. *Chem. Phys. Lett.* **2013**, *577*, 6−10.
(20) Bauzá, A.; Frontera, A. Aerogen Bonding Interaction: A New Supramolecular Force? *Angew. Chem., Int. Ed.* **2015**, *54* (25), 7340−7343.
(21) Arunan, E.; Desiraju, G. R.; Klein, R. A.; Sadlej, J.; Scheiner, S.; Alkorta, I.; Clary, D. C.; Crabtree, R. H.; Dannenberg, J. J.; Hobza, P.; Kjaergaard, H. G.; Legon, A. C.; Mennucci, B.; Nesbitt, D. J. Definition of the hydrogen bond (IUPAC Recommendations 2011). *Pure Appl. Chem.* **2011**, *83* (8), 1637.
(22) Arunan, E.; Desiraju, G. R.; Klein, R. A.; Sadlej, J.; Scheiner, S.; Alkorta, I.; Clary, D. C.; Crabtree, R. H.; Dannenberg, J. J.; Hobza, P.; Kjaergaard, H. G.; Legon, A. C.; Mennucci, B.; Nesbitt, D. J. Defining the hydrogen bond: An account (IUPAC Technical Report). *Pure Appl. Chem.* **2011**, *83* (8), 1619.
(23) Moore, T. S.; Winmill, T. F. CLXXVII.—The state of amines in aqueous solution. *J. Chem. Soc., Trans.* **1912**, *101* (0), 1635−1676.
(24) Latimer, W. M.; Rodebush, W. H. Polarity and Ionization from the Standpoint of the Lewis Theory of Valence. *J. Am. Chem. Soc.* **1920**, *42* (7), 1419−1433.
(25) Scheiner, S. Forty years of progress in the study of the hydrogen bond. *Struct. Chem.* **2019**, *30* (4), 1119−1128.
(26) Kass, S. R. Zwitterion−Dianion Complexes and Anion−Anion Clusters with Negative Dissociation Energies. *J. Am. Chem. Soc.* **2005**, *127* (38), 13098−13099.
(27) Mata, I.; Alkorta, I.; Molins, E.; Espinosa, E. Electrostatics at the Origin of the Stability of Phosphate-Phosphate Complexes Locked by Hydrogen Bonds. *ChemPhysChem* **2012**, *13* (6), 1421−1424.
(28) Mata, I.; Alkorta, I.; Molins, E.; Espinosa, E. Tracing environment effects that influence the stability of anion−anion complexes: The case of phosphate−phosphate interactions. *Chem. Phys. Lett.* **2013**, *555*, 106−109.
(29) Mata, I.; Molins, E.; Alkorta, I.; Espinosa, E. The Paradox of Hydrogen-Bonded Anion−Anion Aggregates in Oxoanions: A Fundamental Electrostatic Problem Explained in Terms of Electrophilic···Nucleophilic Interactions. *J. Phys. Chem. A* **2015**, *119* (1), 183−194.
(30) Alkorta, I.; Mata, I.; Molins, E.; Espinosa, E. Charged versus Neutral Hydrogen-Bonded Complexes: Is There a Difference in the Nature of the Hydrogen Bonds? *Chem. - Eur. J.* **2016**, *22* (27), 9226−9234.
(31) Alkorta, I.; Mata, I.; Molins, E.; Espinosa, E. Energetic, Topological and Electric Field Analyses of Cation-Cation Nucleic Acid Interactions in Watson-Crick Disposition. *ChemPhysChem* **2019**, *20* (1), 148−158.
(32) Shokri, A.; Ramezani, M.; Fattahi, A.; Kass, S. R. Electrostatically Defying Cation−Cation Clusters: Can Likes Attract in a Low-Polarity Environment? *J. Phys. Chem. A* **2013**, *117* (38), 9252−9258.
(33) Weinhold, F.; Klein, R. A. Anti-Electrostatic Hydrogen Bonds. *Angew. Chem., Int. Ed.* **2014**, *53* (42), 11214−11217.
(34) Frenking, G.; Caramori, G. F. No Need for a Re-examination of the Electrostatic Notation of the Hydrogen Bonding: A Comment. *Angew. Chem., Int. Ed.* **2015**, *54* (9), 2596−2599.
(35) Chalanchi, S. M.; Alkorta, I.; Elguero, J.; Quiñonero, D. Hydrogen Bond versus Halogen Bond in Cation−Cation Complexes: Effect of the Solvent. *ChemPhysChem* **2017**, *18* (23), 3462−3468.
(36) Prohens, R.; Portell, A.; Font-Bardia, M.; Bauzá, A.; Frontera, A. H-Bonded anion−anion complex trapped in a squaramido-based receptor. *Chem. Commun.* **2018**, *54* (15), 1841−1844.
(37) Weinhold, F. Theoretical Prediction of Robust Second-Row Oxyanion Clusters in the Metastable Domain of Antielectrostatic Hydrogen Bonding. *Inorg. Chem.* **2018**, *57* (4), 2035−2044.
(38) Iribarren, Í.; Montero-Campillo, M. M.; Alkorta, I.; Elguero, J.; Quiñonero, D. Cations brought together by hydrogen bonds: the protonated pyridine−boronic acid dimer explained. *Phys. Chem. Chem. Phys.* **2019**, *21* (10), 5796−5802.
(39) Khan, S.; Roy, S.; Harms, K.; Bauzá, A.; Frontera, A.; Chattopadhyay, S. Observation of an anion···anion interaction in a square planar copper(II) Schiff base complex: DFT study and CSD analysis. *Inorg. Chim. Acta* **2019**, *487*, 465−472.
(40) Lamberts, K.; Handels, P.; Englert, U.; Aubert, E.; Espinosa, E. Stabilization of polyiodide chains via anion···anion interactions: experiment and theory. *CrystEngComm* **2016**, *18* (21), 3832−3841.
(41) Quiñonero, D.; Alkorta, I.; Elguero, J. Cation−cation and anion−anion complexes stabilized by halogen bonds. *Phys. Chem. Chem. Phys.* **2016**, *18* (40), 27939−27950.
(42) Wang, G.; Chen, Z.; Xu, Z.; Wang, J.; Yang, Y.; Cai, T.; Shi, J.; Zhu, W. Stability and Characteristics of the Halogen Bonding Interaction in an Anion−Anion Complex: A Computational Chemistry Study. *J. Phys. Chem. B* **2016**, *120* (4), 610−620.
(43) Wang, C.; Danovich, D.; Shaik, S.; Wu, W.; Mo, Y. Attraction between electrophilic caps: A counterintuitive case of noncovalent interactions. *J. Comput. Chem.* **2019**, *40* (9), 1015−1022.
(44) Zhu, Z.; Wang, G.; Xu, Z.; Chen, Z.; Wang, J.; Shi, J.; Zhu, W. Halogen bonding in differently charged complexes: basic profile, essential interaction terms and intrinsic σ-hole. *Phys. Chem. Chem. Phys.* **2019**, *21*, 15106.
(45) He, Q.; Kelliher, M.; Bähring, S.; Lynch, V. M.; Sessler, J. L. A Bis-calix[4]pyrrole Enzyme Mimic That Constrains Two Oxoanions in Close Proximity. *J. Am. Chem. Soc.* **2017**, *139* (21), 7140−7143.
(46) Mungalpara, D.; Valkonen, A.; Rissanen, K.; Kubik, S. Efficient stabilisation of a dihydrogenphosphate tetramer and a dihydrogenpyrophosphate dimer by a cyclic pseudopeptide containing 1,4-disubstituted 1,2,3-triazole moieties. *Chem. Sci.* **2017**, *8* (9), 6005−6013.
(47) Fatila, E. M.; Pink, M.; Twum, E. B.; Karty, J. A.; Flood, A. H. Phosphate−phosphate oligomerization drives higher order co-assemblies with stacks of cyanostar macrocycles. *Chem. Sci.* **2018**, *9* (11), 2863−2872.
(48) Sabater, P.; Zapata, F.; Caballero, A.; Alkorta, I.; Ramirez de Arellano, C.; Elguero, J.; Molina, P. Synthesis, Structure and Anion Sensing Properties of a Dicationic Bis(imidazolium)-Based Cyclophane. *ChemistrySelect* **2018**, *3* (13), 3855−3859.
(49) Fatila, E. M.; Twum, E. B.; Sengupta, A.; Pink, M.; Karty, J. A.; Raghavachari, K.; Flood, A. H. Anions Stabilize Each Other inside Macrocyclic Hosts. *Angew. Chem., Int. Ed.* **2016**, *55* (45), 14057−14062.
(50) Sheetz, E. G.; Qiao, B.; Pink, M.; Flood, A. H. Programmed Negative Allostery with Guest-Selected Rotamers Control Anion−Anion Complexes of Stackable Macrocycles. *J. Am. Chem. Soc.* **2018**, *140* (25), 7773−7777.
(51) Zhao, W.; Qiao, B.; Chen, C.-H.; Flood, A. H. High-Fidelity Multistate Switching with Anion−Anion and Acid−Anion Dimers of Organophosphates in Cyanostar Complexes. *Angew. Chem., Int. Ed.* **2017**, *56* (42), 13083−13087.
(52) González, L.; Zapata, F.; Caballero, A.; Molina, P.; Ramírez de Arellano, C.; Alkorta, I.; Elguero, J. Host−Guest Chemistry: Oxoanion Recognition Based on Combined Charge-Assisted C−H or Halogen-Bonding Interactions and Anion···Anion Interactions Mediated by Hydrogen Bonds. *Chem. - Eur. J.* **2016**, *22* (22), 7533−7544.
(53) Zhao, W.; Qiao, B.; Tropp, J.; Pink, M.; Azoulay, J. D.; Flood, A. H. Linear Supramolecular Polymers Driven by Anion−Anion Dimerization of Difunctional Phosphonate Monomers Inside Cyanostar Macrocycles. *J. Am. Chem. Soc.* **2019**, *141* (12), 4980−4989.
(54) Geerlings, P.; De Proft, F.; Langenaeker, W. Conceptual Density Functional Theory. *Chem. Rev.* **2003**, *103* (5), 1793−1874.
(55) Azofra, L. M.; Alkorta, I.; Elguero, J.; Toro-Labbé, A. Mechanisms of Formation of Hemiacetals: Intrinsic Reactivity Analysis. *J. Phys. Chem. A* **2012**, *116* (31), 8250−8259.
(56) Azofra, L. M.; Alkorta, I.; Toro-Labbé, A.; Elguero, J. Modeling the mechanism of glycosylation reactions between ethanol, 1,2-

https://dx.doi.org/10.1021/acs.jpca.9b10681
J. Phys. Chem. A 2020, 124, 2207−2214

ethanediol and methoxymethanol. *Phys. Chem. Chem. Phys.* **2013**, *15* (33), 14026−14036.
(57) Qiu, S.; Azofra, L. M.; MacFarlane, D. R.; Sun, C. Why is a proton transformed into a hydride by [NiFe] hydrogenases? An intrinsic reactivity analysis based on conceptual DFT. *Phys. Chem. Chem. Phys.* **2016**, *18* (22), 15369−15374.
(58) Martínez, J.; Toro-Labbé, A. The reaction force. A scalar property to characterize reaction mechanisms. *J. Math. Chem.* **2009**, *45* (4), 911−927.
(59) Toro-Labbé, A.; Gutiérrez-Oliva, S.; Murray, J. S.; Politzer, P. The reaction force and the transition region of a reaction. *J. Mol. Model.* **2009**, *15* (6), 707−710.
(60) Politzer, P.; Reimers, J. R.; Murray, J. S.; Toro-Labbé, A. Reaction Force and Its Link to Diabatic Analysis: A Unifying Approach to Analyzing Chemical Reactions. *J. Phys. Chem. Lett.* **2010**, *1* (19), 2858−2862.
(61) Cárdenas-Jirón, G. I.; Gutiérrez-Oliva, S.; Melin, J.; Toro-Labbé, A. Relations between Potential Energy, Electronic Chemical Potential, and Hardness Profiles. *J. Phys. Chem. A* **1997**, *101* (25), 4621−4627.
(62) Toro-Labbé, A. Characterization of Chemical Reactions from the Profiles of Energy, Chemical Potential, and Hardness. *J. Phys. Chem. A* **1999**, *103* (22), 4398−4403.
(63) Echegaray, E.; Toro-Labbé, A. Reaction Electronic Flux: A New Concept To Get Insights into Reaction Mechanisms. Study of Model Symmetric Nucleophilic Substitutions. *J. Phys. Chem. A* **2008**, *112* (46), 11801−11807.
(64) Chattaraj, P. K.; Sarkar, U.; Roy, D. R. Electrophilicity Index. *Chem. Rev.* **2006**, *106* (6), 2065−2091.
(65) Morell, C.; Herrera, B.; Gutiérrez-Oliva, S.; Cerón, M.-L.; Grand, A.; Toro-Labbé, A. A Relation between Different Scales of Electrophilicity: Are the Scales Consistent Along a Chemical Reaction? *J. Phys. Chem. A* **2012**, *116* (26), 7074−7081.
(66) Zhao, Y.; Truhlar, D. G. The M06 suite of density functionals for main group thermochemistry, thermochemical kinetics, noncovalent interactions, excited states, and transition elements: two new functionals and systematic testing of four M06-class functionals and 12 other functionals. *Theor. Chem. Acc.* **2008**, *120* (1), 215−241.
(67) Ditchfield, R.; Hehre, W. J.; Pople, J. A. Self-Consistent Molecular-Orbital Methods. IX. An Extended Gaussian-Type Basis for Molecular-Orbital Studies of Organic Molecules. *J. Chem. Phys.* **1971**, *54* (2), 724−728.
(68) Klamt, A.; Schüürmann, G. COSMO: a new approach to dielectric screening in solvents with explicit expressions for the screening energy and its gradient. *J. Chem. Soc., Perkin Trans. 2* **1993**, No. 5, 799−805.
(69) Valiev, M.; Bylaska, E. J.; Govind, N.; Kowalski, K.; Straatsma, T. P.; Van Dam, H. J. J.; Wang, D.; Nieplocha, J.; Apra, E.; Windus, T. L.; de Jong, W. A. NWChem: A comprehensive and scalable open-source solution for large scale molecular simulations. *Comput. Phys. Commun.* **2010**, *181* (9), 1477−1489.
(70) Serjeant, E. P.; Dempsey, B. *Ionisation Constants of Organic Acids in Aqueous Solution*; International Union of Pure and Applied Chemistry (IUPAC): 1979.
(71) Alkorta, I.; Elguero, J.; Cintas, P. Adding Only One Priority Rule Allows Extending CIP Rules to Supramolecular Systems. *Chirality* **2015**, *27* (5), 339−343.
(72) Alkorta, I.; Elguero, J. Self-Discrimination of Enantiomers in Hydrogen-Bonded Dimers. *J. Am. Chem. Soc.* **2002**, *124* (7), 1488−1493.
(73) Picazo, O.; Alkorta, I.; Elguero, J. Large Chiral Recognition in Hydrogen-Bonded Complexes and Proton Transfer in Pyrrolo[2,3-b]pyrrole Dimers as Model Compounds. *J. Org. Chem.* **2003**, *68* (19), 7485−7489.
(74) Parr, R. G.; Chattaraj, P. K. Principle of maximum hardness. *J. Am. Chem. Soc.* **1991**, *113* (5), 1854−1855.

https://dx.doi.org/10.1021/acs.jpca.9b10681
J. Phys. Chem. A 2020, 124, 2207−2214